Journal homepage www.jzs.uos.edu.krd
**Journal of ZankoiSulaimani**
Part-A- (Pure and Applied Sciences)

# First principle structural and electronic properties of $Sr_3Sb_2$ compound of the cubic Phase

Muhamad Hamad Abdullah[1], Matin. Sedighi[1], Mazin Sherzad Othman[1], Behroz Mahmodi[1]

*1 Department of General Science, Faculty of Education, Soran University, Soran-Erbil, Iraq*
*Email: matin.sedighi@soran.edu.iq*

**Article info**

Original: 10 May 2015
Revised: 17 June 2015
Accepted: 25 June 2015
Published online:
20 Dec. 2015

***Key Words:***
*DFT,*
*Band structure, electronic properties, structural properties,*
*effective mass*

**Abstract**

The structural and electronic properties of $Sr_3Sb_2$ at ambient and under hydrostatic pressure have been calculated using the full potential linear augmented plane wave (FP-LAPW) method. We calculated lattice constant, bulk modulus, the derivative of bulk modulus, cohesive energy, energy, band gap and density of state by using GGA96 method for exchange-correlation. Also, for calculating band structure we used GGA96 and EV-GGA on ambient and under hydrostatic pressure. The magnitude of the gap by GGA96 method is 1.51eV and by EV-GGA is 2.28eV. By fitting the data around the conduction band minimum and the valence band maximum, we find the effective mass of electron and hole of this compound.

## Introduction

Electronic band structure of semiconductors plays a key role in determining their properties and applications in various devices such as lasers, detectors, integrated circuits, etc. The combination of Sr with the fifth group elements of periodic table produces semiconductor compounds. In past works, we investigated some combinations of II and V elements [1-5]. Phase diagram of strontium and antimony combination was investigated at different temperatures [6]. It was found that strontium and antimony combinations are formed in the $Sr_3Sb_2$, $Sr_{11}Sb_{10}$, $Sr_5Sb_4$, $Sr_2Sb_3$ and $SrSb_3$ systems. Wyckoff [8] stated that the phase diagram of $Sr_3Sb_2$ is quite similar to that of calcium antimonite. Thus, since we know $Ca_3Sb_2$ does exist and it has cubic and hexagonal phases, we conclude the same for $Sr_3Sb_2$. Moreover, based on melting point data, we know that the compound can be found as a solid. However, we will calculate the cohesive energy to show that $Sr_3Sb_2$ is stable and can exist. So, $Sr_3Sb_2$ crystallizes into two different phases in both body center cubic (bcc) and hexagonal structures. We investigated hexagonal phase in a previous work [7]. In this work, we investigate the structural and electronic properties of the cubic phase for this compound. The atomic position of the cubic phase of $Sr_3Sb_2$ are similar to those of $(Fe, Mn)_2O_3$ with the space group of Ia-3 (206) [8]. We make use of Density Functional Theory (DFT) [9-10] to investigate it, but there is no report on the structural and electronic properties of $Sr_3Sb_2$.

The rest of the paper is organized as follows: Section 2 gives the details of the computational method and some important parameters. Next we present our results in section 3. Finally we conclude our calculations.

## Computational detail

The calculations were performed in the framework of density functional theory. We have employed the full potential linearized augmented plane wave (FP-LAPW) method as implemented in the WIEN2K code [11] that has been shown to yield reliable results for the electronic and structural properties of various solids. Energy calculation in the computation of material properties is the key role. In density functional theory, Hohenberg and Kohn [9] have shown that the electron density $\rho(r)$ uniquely defines the total energy $E_{tot}$of a system and is a functional of the density, $E_{tot}(\rho)$:

$$E_{tot} = T_s(\rho) + E_{ee}(\rho) + E_{eN}(\rho) + E_{xc}(\rho) + E_{NN} \quad (1)$$

The different electronic contributions are conventionally labeled as, respectively, the kinetic energy (of the non-interacting particles), the electron–electron repulsion, nuclear–electron attraction and exchange correlation energies. The last term corresponds to the repulsive Coulomb energy of the fixed nuclei $E_{NN}$.

In the FP-LAPW approach [12] the wave function, charge density and potential are expanded differently in the two regions of the unit cell, Figure 1. Inside the non-overlapping spheres within the muffin-tin radius (RMT) around each atom, spherical harmonics expansions are used, while in the remaining space of the unit cell a plane wave basis set is chosen.

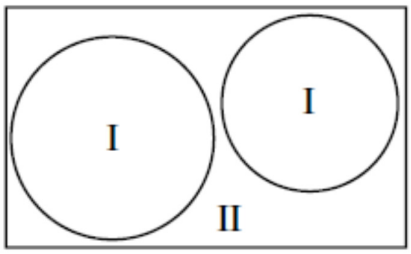


Figure-1: Partitioning of the unit cell into atomic spheres (I) and an interstitial region (II).

Potential within atomic spheres is expanded in the form:

$$V(\vec{r}) = \sum_{lm} V_{lm}(\vec{r}) Y_{lm}(\hat{r}) \quad (2)$$

and outside of these spheres (in interstitial region) as:

$$V(\vec{r}) = \sum_{K} V_{\vec{K}} e^{i\vec{K}.\vec{r}} \quad (3)$$

where $Y_{lm}(\hat{r})$ correspond to spherical lattice harmonics.

Then, variation of $E_{tot}$ gives a set of effective one-particle Schrodinger equations (written for an atom in Rydberg atomic units), the so-called Kohn–Sham equations [10]:

$$\{-\nabla^2 + V_{Ne} + V_{ee} + V_{xc}\}\chi_{ik} = \epsilon_{ik}\chi_{ik} \quad (4)$$

which must be solved. Kohn–Sham wave functions are expanded in terms of spherical harmonic functions inside the non-overlapping muffin-tin spheres surrounding the atomic sites (MT spheres) and in the interstitial region, the wave functions are expanded in plane waves. The exchange-correlation potential for structural properties was calculated by generalized gradient approximation (GGA96) based on Perdew et al.[13], while for electronic properties in addition to that, Engel and Vosko scheme (EV-GGA) [14] was also applied.

The muffin-tin radii RMT were assumed to be 2.5 for Sr and Sb atoms. The maximum $l$ value for the wave function expansions inside spheres was confined to $l_{max} = 10$. The plane wave cut-off of $K_{max}$ = 8.0/RMT is chosen for the expansion of the wave functions in the interstitial region, while the charge density was Fourier expanded up to $G_{max}$ = 12(Ryd) and 500 k-points were sampled in the irreducible wedge of the first Brillouin zone for body center cubic which correspond to 7×7×7 grids in Monkhorst-Park scheme [15].

## Results and discussion

### *A. Structural Properties*

The $Sr_3Sb_2$ compound is crystallized in both the cubic and hexagonal structures with the space group of Ia-3 and P3m1, respectively. In a past work, we investigate hexagonal phase [7]. $Sr_3Sb_2$ has 40 atoms per primitive cell. In this primitive cell, the Sb atoms have two types of symmetries, called Sb1 and Sb2 with 4 and 12 members, respectively. The Sr, Sb1 and Sb2 atoms in this phase are at (x, y, z, etc.), (1/4, 1/4, 1/4, etc.) and (u, 0, 1/4, etc.) positions respectively [8]. Sb1 atoms have 6 atoms on vicinity with same distance, but Sb2 atoms have 6 atoms on vicinity which division to three groups and distances are slightly different. Figure 2 illustrates the positions of $Sr_3Sb_2$ unit cell atoms in the cubic phase. In the first step, we calculated the optimized values of the lattice and internal parameters.

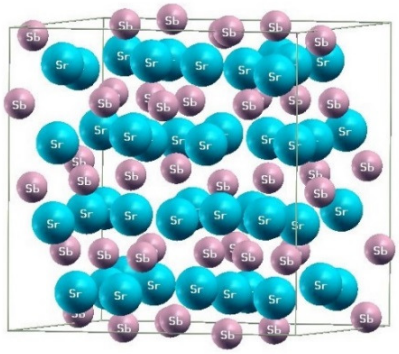


Figure-2: Unit cell of $Sr_3Sb_2$ and atoms positions in body center structure.

Figure 3 shows the total energy of this compound as a function of volume. The curve was obtained by calculating the total energy $E_{tot}$ at many different volumes around equilibrium and by fitting the calculated values to the Murnaghan's equation of state [16].

$$E_{tot}(V) = \frac{BV}{B\prime}\left[\frac{\left(\frac{V_0}{V}\right)^{B'}}{B'-1} + 1\right] + E_0 - \frac{V_0 B}{B'-1} \quad (5)$$

where B is bulk modulus defined by the following [17]:

$$B = -V\left(\frac{\partial P}{\partial V}\right) = V\frac{d^2E_{tot}}{dV^2} \quad (6)$$

$B'$ is the derivative of bulk modulus

$$B' = \left(\frac{\partial B}{\partial P}\right)_T \quad (7)$$

and pressure can be obtained from:

$$P(V) = \frac{B}{B\prime}\left[\left(\frac{V_0}{V}\right)^{B'} - 1\right] \quad (8)$$

where $V$ and $V_0$ represent the atomic volume at pressure P and its value at zero pressure, respectively. In order to optimize the internal parameters, the atomic positions inside a primitive cell are relaxed within the scheme of Hellman–Feynman [18]. By using the energy curve in terms of volume, the values of the optimized parameters of the lattice, the bulk modulus and the derivative of bulk modulus were calculated. The results are summarized in Tables 1.

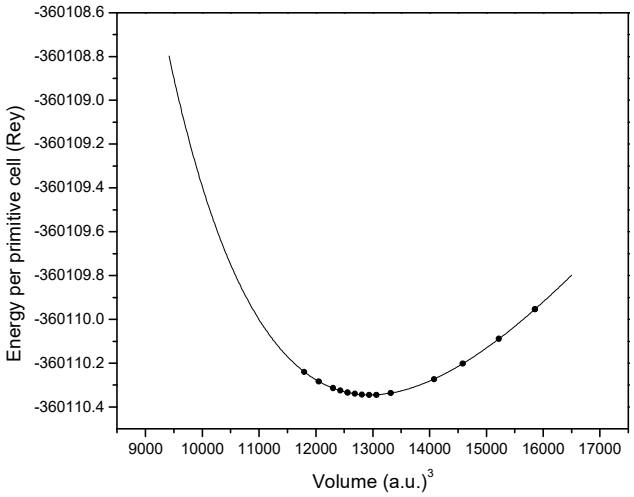


Figure-3: Calculated total energy as a function of primitive cell volume of $Sr_3Sb_2$.

The cohesive energy is defined as the difference between the energy of an isolated atom and the energy of the same atom in the solid [19]. Cohesive energy has also been calculated and its magnitude is given in Table 2.

Table-1: Four internal parameters (u, x, y, z) in cubic structure of $Sr_3Sb_2$.

| | Parameters | Our calculated parameters |
|---|---|---|
| Cubic | x, y, z | 0.3788, 0.1468, 0.3837 |
| | u | 0.9648 |

Table-2: Lattice parameters, bulk modulus (B), its pressure derivative (B'), band length and cohesive energy per formula unit obtained using FP-LAPW calculations within GGA96 for $Sr_3Sb_2$.

| | **Parameters** | **Present work** |
|---|---|---|
| Lattice parameter | a=b=c $(a.u.)$ | 29.588245 |
| Bulk medlous | B $(GPa)$ | 25.2299 |
| Derivative of bulk medulos | B' | 4.4936 |
| Cohesive Energy | $E_{cohsive}$ (Ryd) | 1.513 |
| Bond length | Sr-Sb1(A) | 3.32601 |
| | Sr-Sb2(A) | 3.23192, 3.38867, 3.43911 |

## *B. Electronic Properties*

In this section, we study the electronic properties of $Sr_3Sb_2$ in the cubic phase using the obtained optimized values of lattice parameters and atoms positions. Figure 4 shows the band structures of $Sr_3Sb_2$ at ambient pressure by using GGA96 and EV-GGA methods. Energy band gap value, anti-symmetric gap (Eg−A: the energy gap between two parts of the valence bands) and the valence bands which for this case is separated into two sub bands that are labeled starting from the top as VB1 and VB2 thus calculated are given in Table 3.

Table-3: Calculated values of the band gap, band widths (VB1 and VB2) and the anti-symmetry gap of $Sr_3Sb_2$ in the bcc phase

| Method | Eg (eV) | VB1 (eV) | VB2 (eV) | Anti-symmetry-gap (eV) |
|---|---|---|---|---|
| GGA96 | 1.51 | 1.52 | 0.44 | 5.50 |
| EV-GGA | 2.28 | 1.33 | 0.41 | 5.55 |

The specified gap by these two methods is of the type $N \rightarrow \Gamma$.

We studied effects of applying pressure on the band gap, anti-symmetry gap and bandwidths by applying Eq.(8). Figures 5 and 6 show results of applying pressure using GGA96 and EV-GGA methods. According to figure 5, we can say that the bandwidth increases with the pressure which is due to the Pauli Exclusion Principle and is the increase of overlap.

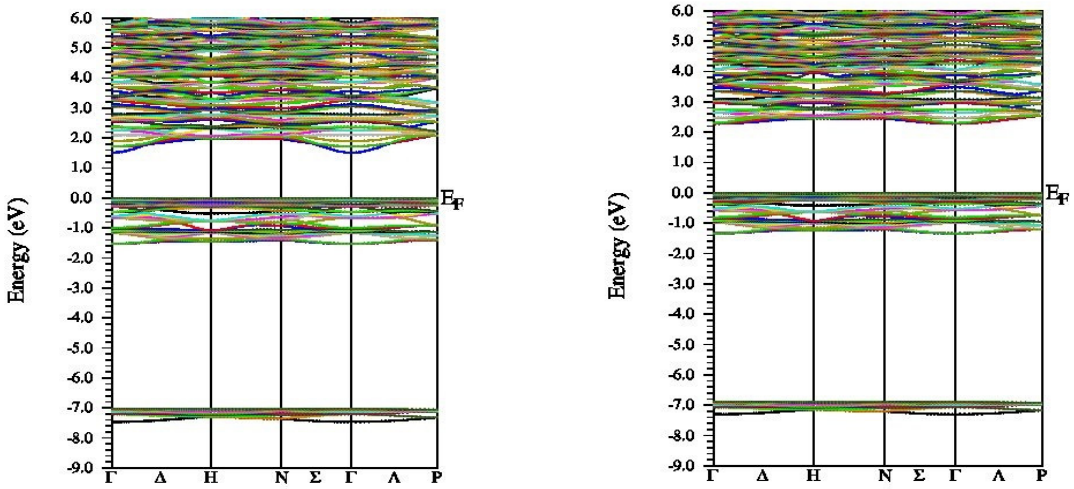


Figure-4: Band structure calculated along high symmetry directions for the cubic phase within the GGA96 (left) and EV-GGA (right).

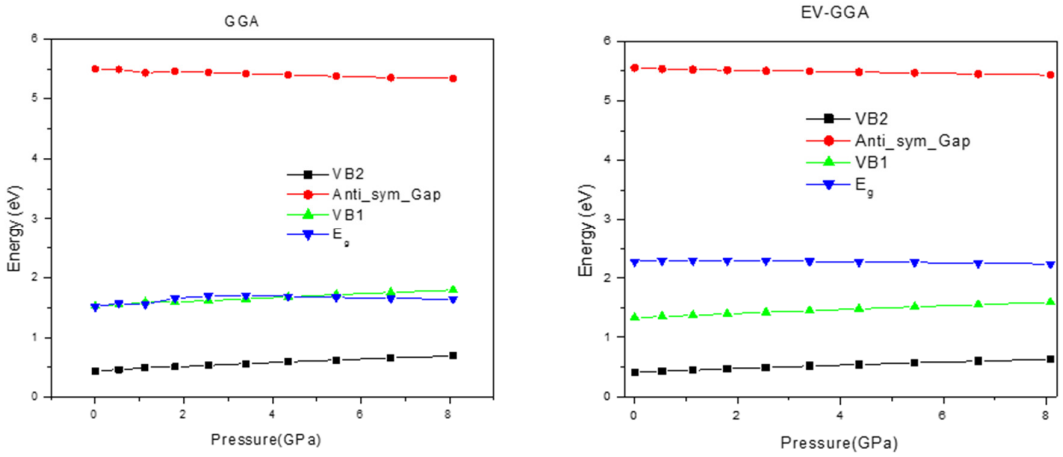


Figure-5: The behavior of the band gap ($E_g$), valence bandwidths and anti-symmetric gap, $E_{g-A}$, for $Sr_3Sb_2$ using both GGA96 and EV-GGA methods at different pressure.

Also, we investigated the effective masses of electrons and holes. The effective masses of electrons and holes are calculated under ambient condition. Since $Sr_3Sb_2$ is a semiconductor, then its effective mass for electron as well as holes were obtained from the E-k diagram around the conduction band minimum and the valence band maximum by a parabola. We are interested in studying the effective masses of electrons and holes, which are important for the excitonic, optical, thermal and conduction properties of matter properties. We have computed the effective masses of electrons and holes about Γ and *N* points using GGA96 and EV-GGA methods. The different effective masses are obtained from the equation

$$m^* = \frac{\hbar^2}{(\frac{d^2E}{dk^2})} \qquad (9)$$

We fitted the data around maximum and minimum points with the above well-known equation Eq. (9). Figs (6 and 7) show our fit. Electrons and holes effective masses are 0.238 and 9.912 and 1.21 and 8.614 in GGA96 and EV-GGA, respectively. We usually report $\frac{m^*}{m_e}$ for the calculated effective mass.

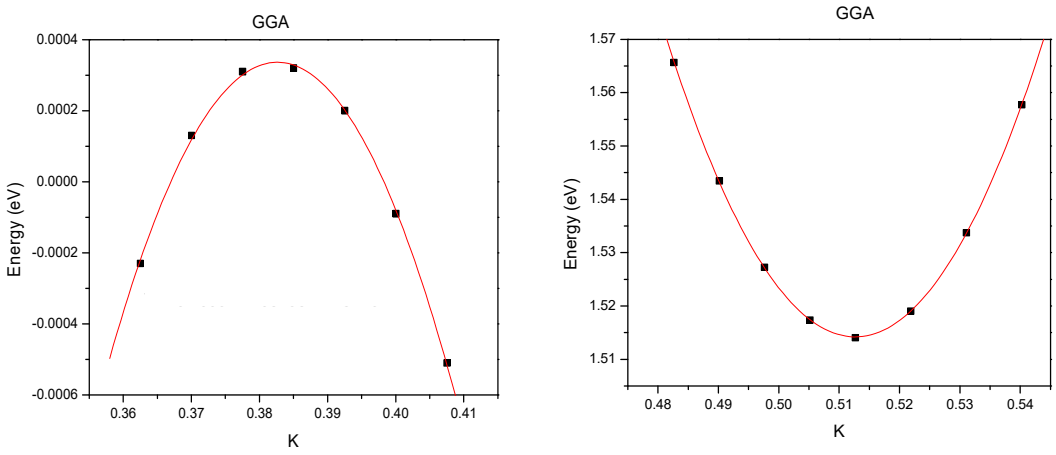


Figure-6: fitting the actual E-k diagram around the conduction band minimum and the valence band maximum in GGA96 method.

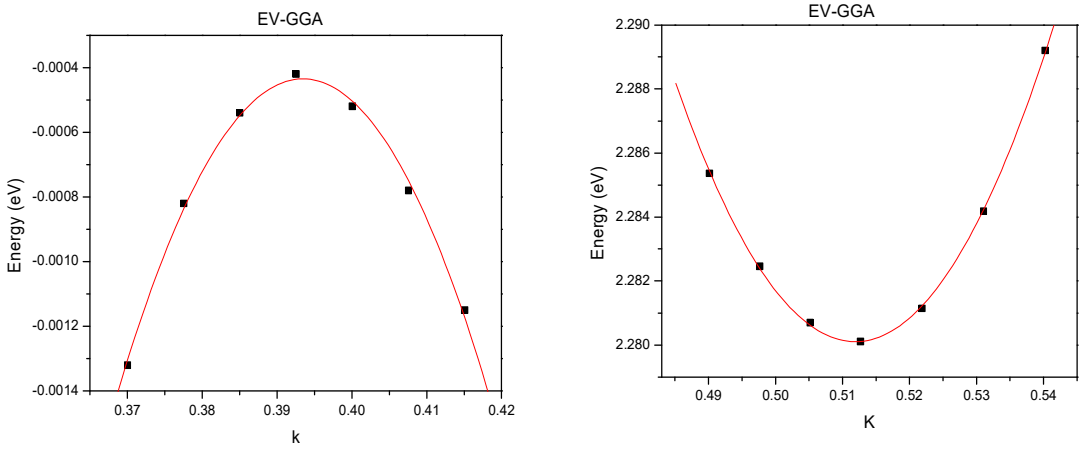


Figure 7: Fitting the actual E-k diagram around the conduction band minimum and the valence band maximum in EV-GGA method.

For further study of the electronic structure of this compound, the total and partial densities of states (DOS) are computed at the equilibrium lattice constant by the tetrahedral method [20] using GGA96. The corresponding results are plotted in figure 8.

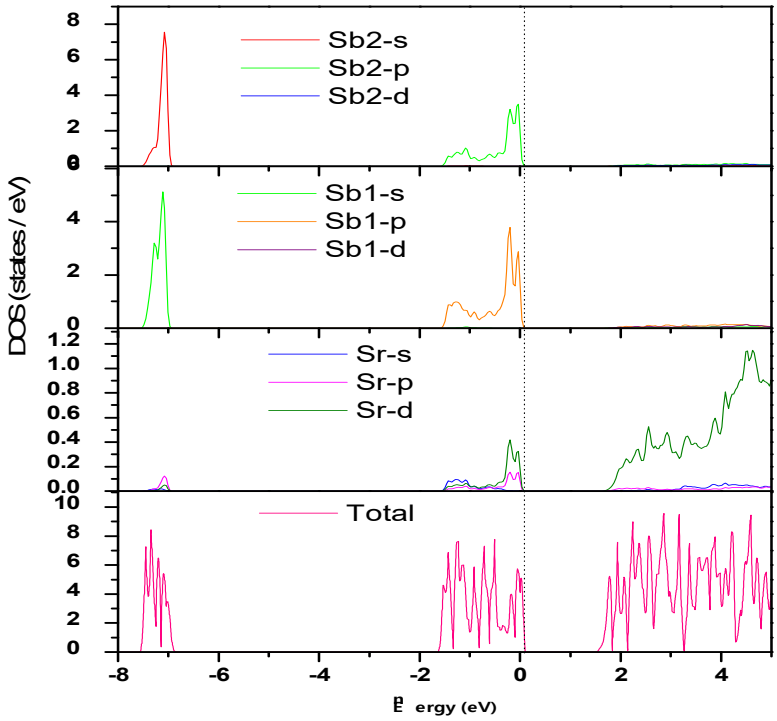


Figure-8: Calculated partial DOS for each atom in $Sr_3Sb_2$ compound.

## Conclusion

In this work, for the first time, we calculated the lattice parameters of cubic $Sr_3Sb_2$, which are a=b=c=29.588a.u. Also, the semiconducting energy gap obtained for cubic $Sr_3Sb_2$ is 2.28eV, which seems the gap changes by using pressure in EV-GGA method is linearly. We also find effective mass of electron and hole by fitting the actual E-k diagram around the conduction band minimum and the valence band maximum for this compound.

## References

[1] Mokhtari, A. "*Density Functional Study of the Group II Phosphide Semiconductor Compounds under Hydrostatic Pressure*" J. Phys: Condens. Matter 20, pp. 135224, (2008).

[2] Mokhtari, A. and M, Sedighi. "*The Effect of Hydrostatic Pressure on the Physical Properties of Magnesium Arsenide in Cubic and Hexagonal Phases*" Physica B 405, pp. 1715, (2010).

[3] Sedighi, M. Arghavani Nia, B. H. Zarringhalam, H and Moradian, R. "*First Principles Investigation of Magnesium Antimonite Semiconductor Compound in Two Different Phases under Hydrostatic Pressure*" Physica B 406, pp. 3149, (2011).

[4] Sedighi, M, Arghavani Nia, B. Zarringhalam, H. and Moradian, R. "*Density Functional Theory Study of the Structural and Electronic Properties of Mg3Bi2 in Hexagonal and Cubic Phases*" Eur. Phys. J. Appl. Phys. 61, pp. 10103, (2013).

[5] Arghavani Nia, B. Sedighi, M. Shahrokhi, M. and Moradian, R. "*Ab initio density functional theory investigation of the structural, electronic and optical properties of Ca3Sb2 in hexagonal and cubic phases*" Journal of Solid State Chemistry France, 207, pp. 140-146, (2013).

[6] Ropp, R. C. "*Encyclopedia of the Alkaline Earth Compounds*" Elsevier Science, pp. 324, (2012).

[7] M. Sedighi, M. Danesh, S. Vaji. "*First-principles investigation of the structural and electronic properties of Sr3Sb2 in hexagonal phase*" JZS-A, pp.169, (2013)

[8] Wyckoff,R. W. G. "*Crystal Structures*", 2nd Ed. Krieger, Malabar, FL, pp. 5 (1986).
[9] Hohenberg, P. and Kohn, W. "*Inhomogeneous Electron Gas*" Phys. Rev. 136, pp. B864, (1964).
[10] Kohn, W. and Sham, L. J. "Self-Consistent Equations Including Exchange and Correlation Effects" Phys. Rev. 140, pp. A1133 (1965).
[11] Blaha, P. Schwarz, Madsen, K.G.K.H. Vasnicka, D.K. and Luitz, J. WIEN2K, "*An Augmented Plane Wave + Local Orbitals Program for Calculating Crystal Properties*", Karlheinz Schwarz, Techn. Universitat Wien, Austria, (2001).
[12] Blaha, P. Schwarz, K. Sorantin, P. and Trickey, S. "*Full-potential, linearized augmented plane wave programs for crystalline systems*" Comp. Phys. Commun, 59, pp. 399-415, (1990).
[13] Perdew, J. P. Burke, K. and Ernzerhof, M."*Generalized Gradient Approximation Made Simple*" Phys. Rev. Lett. 77, pp. 3865, (1996).
[14] Engel, E. and Vosko, S. H. "*Exact Exchange-Only Potentials and the Virial Relation as Microscopic Criteria for Generalized Gradient Approximations*" Phys. Rev. B, 47, pp. 13164, (1993).
[15] Monkhorst, H. J. and Park, J. D. "*Special Points for Brillouin-Zone Integrations*" Phys. Rev. B 13, pp. 5188, (1976) .
[16] Murnaghan, F. D. "The compressibility of media under extreme pressure", Proc. Natl. Acad. Sci. USA 30, 244 (1944).
[17] Kittel, C."*Introduction to Solid State Physics*", Wiley, New York, pp. 157 (1976).
[18] Pulay, P. "*Investigation of the Molecular Force Field with the Help of Parameter Representation of Force Constants*" Mol. Phys. 17, pp. 197, (1969).
[19] Hofmann, P. "*Solid State Physics: An Introduction*": Wiley, pp. 25 (2015).
[20] Blochl, P. E. Jepsen, O. and Andersen O. K. "*Improved tetrahedron method for Brillouin-zone integrations*" Phys. Rev. B 49 16223, (1994)